Green Chemistry

PAPER

View Article Online
View Journal

Cite this: DOI: 10.1039/c9gc00387h

Polyhydroxyalkanoate-derived hydrogen-bond donors for the synthesis of new deep eutectic solvents†

Katarzyna Haraźna, [a] Karolina Walas,[b] Patrycja Urbańska,[b] Tomasz Witko,[c] Wojciech Snoch, [a] Agnieszka Siemek, [a] Barbara Jachimska, [a] Marcel Krzan, [a] Bogna D. Napruszewska, [a] Małgorzata Witko, [a] Szczepan Bednarz [b] and Maciej Guzik *[a]

Bacterial polyesters are a well-known group of polymers with excellent biocompability and biodegradability. They are also a renewable source of a wide array of enantiopure (*R*)-3-hydroxycarboxylic acids. In this study, a series of ternary deep eutectic solvent (DES) systems were prepared using a mixture of micro-organism-derived (*R*)-3-hydroxynonanoic and (*R*)-3-hydroxyheptanoic acids in a molar ratio of 7 : 3 as hydrogen-bond donors (HBDs) and selected quaternary ammonium salts as hydrogen-bond acceptors (HBAs), namely choline, 1-ethyl-3-methylimidazolium and tributylmethylammonium chlorides. For comparison, DESs based on aliphatic carboxylic acid analogues, *i.e.* nonanoic and heptanoic acids, were also studied. The systems were characterised by ^{1}H NMR and FT-IR techniques and the formation of hydrogen bonds between the HBDs and HBAs was proved. The thermal properties, including the melting temperatures and thermal stabilities, as well as the polarity and wetting properties were determined by DSC, TGA, the Nile Red method and dynamic contact angle methods, respectively. The viscosity and density were measured over a temperature range of 30–60 °C. Cytotoxicity and biodegradation studies were conducted and revealed the non-toxic character of the choline-based DES. The ability of the DESs to dissolve lignin was also evaluated. The results demonstrated the potential for a new area of application of bacterial polyesters for the synthesis of novel bio-based solvents.

Received 31st January 2019,
Accepted 24th April 2019

DOI: 10.1039/c9gc00387h

rsc.li/greenchem

Introduction

In recent years, there has been an increased interest in green chemistry, leading to the development of new and safe substitutes alongside their manufacturing technologies with the aim of reducing the negative impact of traditional chemical industries. Green technology is actively looking for new solvents that could replace commonly used organic chemicals, which can often be toxic and highly volatile.[1,2] An interesting alternative to such species are deep eutectic solvents (DESs).[3–6]

According to Abbott's classification,[3] DESs are two component systems formed by the mixing of a hydrogen bond acceptor (HBA), most commonly a quaternary ammonium salt (*e.g.* choline chloride), with a metal salt or hydrogen bond donor (HBD), which include alcohols, amides or carboxylic acids, among others. The key property of these systems is a significant decrease of their melting point, in comparison with the melting temperatures of the pure components, whereby DESs at a temperature lower than 100 °C, even at room temperature, are in a liquid form.[3] Later on, the classification of DESs was expanded by Choi and co-workers,[7] who introduced the so-called natural deep eutectic solvents (NADES) as two- or three-components mixtures, composed of polar primary metabolites, *i.e.* choline chloride, natural acids, amino acids, mono- and disaccharides, and in some cases, using water. They demonstrated that quaternary ammonium salts are not a mandatory component of NADES.[7,8] Finally, recently, hydrophobic DESs were developed by Kroon[9] and Marrucho,[10] comprising terpenes, fatty acids and long-chain alcohols, among others.[6] One of the major advantages of DESs over ionic liquids lies in their preparation method, which is straightforward, with 100% atom efficiency, by a simply mixing and melting of HBDs and HBAs. DESs have been used mainly in

[a]*Jerzy Haber Institute of Catalysis and Surface Chemistry Polish Academy of Sciences, Niezapominajek 8, 30-239 Kraków, Poland. E-mail: ncguzik@cyfronet.pl*
[b]*Cracow University of Technology, Department of Biotechnology and Physical Chemistry, Warszawska 24, 31-155, Kraków, Poland*
[c]*Faculty of Physics, Astronomy and Applied Computer Science, Jagiellonian University, Łojasiewicza 11, 30-348, Kraków, Poland*
†Electronic supplementary information (ESI) available. See DOI: 10.1039/c9gc00387h

electrochemical processes,[3] polymers syntheses[11,12] and enzymatic catalysis[13,14] as well as in extraction of bioactive compounds from biomass.[4,5,15–18]

Polyhydroxyalkanoates (PHAs) may be produced from renewable resources, *i.e.* cellulosic biomass, fatty acids, food waste and post-process waste, *i.e.* whey, molasses and sugar cane[19–21] as well as from technological wastes or even conventional plastic.[22] PHAs are accumulated by numerous bacteria as isolated intracellular granules or as network-like extracellular structures.[23] To date, more than 150 monomers of (*R*)-3-hydroxylic acids (HAs)[24] have been identified, which are characterised by a variety of properties depending on their chain length and functional groups.[25,26] HAs derived from the hydrolysis of PHA could be renewable components for the preparation of DESs. Because they are chemically similar to fatty acids, it seems that they could form hydrophobic DESs, as long-chain carboxylic acids do.[9,27–30]

Due to the partial toxicity of some of the components in DESs, research is focused on the development of non-toxic and biodegradable counterparts in order to create NADESs, which are designed by the incorporation of primary metabolites.[4–10] One of the most promising components of DESs is choline chloride due to its common occurrence and biodegradability in aerobic conditions.[31] Other examples of HBAs include imidazole or other quaternary ammonium salts derivatives; however, their full biodegradability still remains an issue.[15,32,33] It is well known that both HBAs and HBDs have a great impact on a particular DES's biodegradability.[26,34] For this reason, it is important to search for new bioactive molecules that could enhance the natural degradation of DESs, and, in our opinion, HAs could meet this requirement.

Here we present, for the first time, the synthesis of a novel family of ternary DESs based on a mixture of (*R*)-3-hydroxylic acids HBDs, derived from a bacterially synthesised polymer – polyhydroxynonanoate, a member of the medium-chain-length polyhydroxyalkanoates family. For the purpose of this study three hydrogen bond acceptors (HBAs) were selected, namely choline chloride ([Ch]Cl), 1-ethyl-3-methylimidazolium chloride ([EMIm]Cl) and tributylmethylammonium chloride ([TBMA]Cl). The DESs were prepared in different ratios of acceptor to donor. Furthermore, they were thoroughly characterised for their physico-chemical properties and compared to their aliphatic counterparts. We also indicate herein their potential uses as green solvents for the extraction of lignocellulosic material.

Experimental

Materials

Polyhydroxynonanoate (PHN) was produced with *Pseudomonas putida* KT2440 strain with nonanoic acid in the fermentation feed as the sole energy and carbon source; extracted with ethyl acetate and then characterised as in our previous manuscript.[35] The polymer was degraded to its monomeric units *via* an acidic methanolysis, followed by saponification with LiOH[36] to yield free hydroxy fatty acids (HAs) – a mixture of (*R*)-3-hydroxynonanoic and (*R*)-3-hydroxyheptanoic acids in molar ratio of 7 : 3. Choline chloride ([Ch]Cl), 1-ethyl-3-methylimidazolium chloride ([EMIm]Cl) and tributylmethylammonium chloride ([TBMA]Cl) were purchased from Merck, Poland, and were of synthesis grade, similar to the case of all the other chemicals used in this study. A synthetic mixture of aliphatic nonanoic and heptanoic acid in the ratio of 7 : 3 (mol%) was created in order to mimic the (*R*)-3-hydroxyalted fatty acid mixture originating from the PHN polymer. The DESs were constructed by mixing the donor to the acceptor in molar ratios of 1 : 1 or 2 : 1, with heating to 60 °C in order to fasten the solubilisation, and these were then stored at room temperature (r.t.) for further experiments.

Density and viscosity measurements

The densities of the solutions were measured using a DMA 5000 M density meter (Anton Paar), which is based on the oscillating U-tube method. The dynamic and kinematic viscosities were measured using a Lovis 2000 M/ME rolling-ball microviscometer (Anton Paar). This instrument is based on the rolling-ball rule, where a steel ball rolls inside a sample-filled glass capillary. The diameter of the glass capillary was 2.5 mm and was calibrated before the measurements using N100 oil. The apparatus measured viscosity in the range from 0.3 to 10 000 mPa s with an accuracy of 0.05%. All the measurements were conducted in the temperature range of 30–60 °C.

Fourier transform infrared spectroscopy (FT-IR)

FT-IR spectra were recorded on a Nicolet 6700 spectrometer. The spectra of the DESs and organic acids were collected in the range of 4000–650 cm^{-1} at a resolution of 4 cm^{-1} for 64 scans in ATR mode with ZnSe crystal. The spectra of ([TBMA]Cl), ([EMIm]Cl) and ([Ch]Cl) were obtained with KBr pellets in transmission mode (resolution 4 cm^{-1}, 64 scans). All the spectra obtained from the ATR method were normalised to compare them with the spectra obtained by the transmission methods.

Nuclear magnetic resonance (NMR)

The ^{1}H NMR spectra of the synthesised DESs and their individual components were recorded with a Mercury-VX 300 MHz. Each of the samples was dissolved in $CDCl_3$ (~40 mg mL^{-1}), except ([Ch]Cl) : 2HAs DES and ([Ch]Cl), which were dissolved in DMSO-d6 and D_2O, respectively.

Polarity determination

The polarity of the DESs was estimated using the solvatochromic dye Nile Red (NR).[37] Mixtures of 50–100 μL of each DES and 10 μL of the NR solution (0.5 mg mL^{-1} MeOH) were placed into a well plate. Methanol was carefully removed by evaporation under 20–30 mbar at r.t. for 30 min. Next, UV-VIS absorption spectra were collected in the range from 400 to 800 nm. Molar transition energies ($E_{T(NR)}$) were calculated from the following formula:

$$E_T(\mathrm{NR})\ \mathrm{kcal\ mol^{-1}} = hc\nu_{max}N_A = 28\ 591/\lambda_{max}$$

where: h is Planck's constant; c is the speed of the light; ν_{max} is the wave number of maximum absorption; and N_A is Avogadro's constant. A decrease in $E_{T(NR)}$ indicates an increase in polarity.

Thermogravimetric analysis (TGA)

TGA was performed on a Netzsch STA 409 PC Luxx. The samples of about 17.7–22.1 mg were placed in an aluminium oxide crucible and heated in a nitrogen atmosphere at a rate of 10 °C min^{-1} from room temperature to 600 °C.

Differential scanning calorimetry (DSC)

DSC was performed with a Netzsch DSC 204F1 Phoenix instrument, under a nitrogen atmosphere. A sample (4–8 mg) was placed in an aluminium pan sealed with a pierced lid. The temperature was ramped from room temperature to −60 °C at a cooling rate of 5.0 °C min^{-1}, held isothermally for 1 min, and then ramped to 60.0 °C at a heating rate of 5.0 °C min^{-1}, followed by 1 min isotherm. Two cycles were recorded for each sample.

Dynamic contact angle measurements

The dynamic contact angles between the DES and the flat surface of Teflon were measured using a Drop Shape Analyzer KRUSS DSA100M instrument (Hamburg, Germany, Gmbh). Sterile syringe needles (stainless steel, NE 44, KRUSS, Gmbh) were used for each new measurement in automatic mode. The instrument recorded images with a digital camera (200 fps), and were further processed using a digital image processing algorithm to calculate the droplet's contact angle by tangents or by Laplace–Young approximations. Measurements were conducted under constant conditions of temperature (22 ± 0.3 °C) and humidity. For each sample, more than three successive measurements were carried out.

Cytotoxicity test

Sample preparation. All the samples described in this manuscript were tested for their toxic impact on living mammalian cells. Each sample was mixed with cell culture medium to reach a concentration between 100 and 500 μg ml^{-1}. In total, 70 samples containing living MEF 3T3 cells were prepared on multiwall plates. After 24 h of incubation, the cells were removed from the medium, stained and scanned with a fluorescent microscope.

Cell cultures. For the cytotoxicity studies, a mouse embryonic fibroblast cell line was used (Sigma Cat. No. 86052701 3T3 L1 Cell Line from mouse). Cells were grown in plastic culture dishes under sterile conditions in an incubator (Thermo Scientific 8000 Series WJ) maintaining a constant environment (37 °C, 5% CO_2). The medium used was DMEM (Dulbecco's modified Eagle medium) supplemented with 10% fetal bovine serum (FBS) and 1% antibiotics (penicillin and streptomycin) (Sigma Aldrich®). The cell culture was split using a standard passage procedure when the confluence reached approximately 80%. Cells used in the study were after the third, but not beyond the ninth passage.[38]

Cytotoxicity assessment. The fluorescein diacetate/propidium iodide (FDA/PI) test was used to distinguish dead and living cells. The mouse embryonic MEF 3T3 fibroblasts were suspended in PBS. To 0.2 ml of this suspension, a solution of FDA (0.02 μg) and PI (0.6 μg) was added. After 3 min of incubation at room temperature, the fluorescence was observed under a Zeiss Axio Observer Z.1 fluorescent microscope and the percentage of necrotic cells, cells in early apoptosis and the live cells were determined. In order to make an accurate assessment of the impact of the DES solutions on living cells, a tile-scan technique was used to allow imaging of a large sample area at a relatively high magnification. In the experiment, a sample image was made consisting of 121 captures of a single field of view. When using a 10× magnification lens, the final image included cells located on the 200 mm^2 area. Lasers with wavelengths of 488 and 561 nm were used to excite the fluorescent dyes; additionally, a channel of bright field imaging (T-PMT) was switched on to be able to assess whether the stained object was actually a cell.

Biodegradation test

The biodegradation studies were based on principles outlined in the OECD 301 test. Briefly, we adapted the minimal salt medium (MSM) from this method, which was made up as follows: 0.085 g L^{-1} KH_2PO_4, 0.217 g L^{-1} K_2HPO_4, 0.34 g L^{-1} $Na_2HPO_4{\cdot}2H_2O$, 0.005 g L^{-1} NH_4Cl, 0.0364 g L^{-1} $CaCl_2{\cdot}2H_2O$, 0.0225 g L^{-1} $MgSO_4{\cdot}7H_2O$ and 0.00025 g L^{-1} $FeCl_3{\cdot}6H_2O$. Activated sludge (AS) was sourced from Waterworks Karków, Poland. The inoculum (300 ml of AS) was preconditioned in the MSM (700 ml) for a period of 5 days without any carbon source, with vigorous shaking (200 rpm) and at a constant temperature of 20 °C in the dark. For the degradation studies, the DES samples (50 mg L^{-1} in MSM) were inoculated with preconditioned activated sludge (30 mg L^{-1}). The experiments were conducted with vigorous shaking (200 rpm) and at a constant temperature of 20 °C in the dark for 21 days. During that period, the samples were collected and analysed with HPLC-MS as described below.

High-pressure liquid chromatography with mass detection (HPLC-MS)

The analyses were performed by HPLC measurements on an Agilent 1290 Infinity system with an automatic autosampler and MS Agilent 6460 Triple Quad Detector equipped with an Agilent Zorbax Eclipse Plus C18 column (2.1 × 50 mm, 1.8 μm). For separation of the DES's components, the column was eluted at 30 °C at a flow rate of 0.4 mL min^{-1} and developed with a gradient elution of solvent A (10 mM ammonium formate in water) and solvent B (methanol) as follows: 0.00 min (50% A/50% B) to 1.90 min (10% A/90% B) to 1.91 min (50% A/50% B) to 2.60 min (50% A/50% B). The injection interval was 2.6 min. An MS Agilent 6460 Triple Quad tandem mass spectrometer with an Agilent Jet Stream ESI interface was used in negative ion mode for the HBDs and in positive mode for the HBAs. Nitrogen at a flow rate of 10 L min^{-1} was used as the drying gas and for collision-activated

dissociation. The drying gas and sheath gas temperatures were set to 350 °C. The capillary voltage was set to 3500 V, while the nozzle voltage was set to 500 V. Compounds were monitored in multiple reaction monitoring mode (MRM) with the following transitions, polarity, fragmentor (*F*) and collision energies (CE): ESI+: ([EMIm]Cl) 111.1 → 83.1 *m*/*z*, *F* = 102 V, CE = 18 V; ([TBMA]Cl) 200.1 → 58.1 *m*/*z*, *F* = 122 V, CE = 34 V; ([Ch]Cl) 111.1 → 83.1 *m*/*z*, *F* = 98 V, CE = 18 V; ESI−: heptanoic acid 129.1 → 129.1 *m*/*z*, *F* = 78 V, CE = 2 V; nonanoic acid 157.1 → 157.1 *m*/*z*, *F* = 88 V, CE = 2 V; (*R*)-3-hydroxyheptanoic acid 145.1 → 59.1 *m*/*z*, *F* = 73 V, CE = 8 V; (*R*)-3-hydroxynonanoic acid 173.1 → 59.1 *m*/*z*, *F* = 83 V, CE = 10 V. Standard curves were prepared in 50% v/v of solvent A to B and were used for quantitative analysis. MassHunter software (Agilent) was used for HPLC-MS system control, data acquisition and data processing.

Lignin solubility studies

10 mg of lignin (Kraft lignin, Sigma-Aldrich cat. no. 471003) was mixed with a known weight of DES in a range of 150–250 mg, placed in a shaking incubator at 50 °C and then left for 4 days. This followed an estimation of the solubilised lignin by spectrometric measurement at 280 nm; whereby for each particular sample, a blank measurement was deducted by measuring the pure DES absorbance. The concentrations were calculated from the lignin calibration curve obtained in DMSO.

Results and discussion

Deep eutectic solvents' syntheses

Ternary DESs were prepared according to the method described in the M&M section by mixing the HBDs and HBAs in molar ratios of 1 : 1 or 2 : 1. A mixture of (*R*)-3-hydroxylated acids originating from depolymerised polyhydroxynonanoate containing 30 mol% of (*R*)-3-hydroxyheptanoic and 70 mol% of (*R*)-3-hydroxynonanoic acids (herein referred to as HAs), and for comparison purposes, a mixture of nonanoic (70 mol%) and heptanoic (30 mol%) acid, were used as HBDs. We found that, at room temperature, both tributylmethylammonium ([TBMA]Cl) and 1-ethyl-3-methylimidazolium chlorides ([EMIm]Cl) produced liquids with either aliphatic (Aliph) or hydroxy fatty acids (HAs) at both ratios. Interestingly, choline chloride ([Ch]Cl) did not produce a liquid when mixed with aliphatic fatty acids at room temperature, neither did it produce a liquid when reacted at a 1 mol : 1 mol ratio with HAs. However, when the molar ratio was increased to 1 mol ChCl : 2 mol Has, a homogeneous mixture was formed. All of the prepared DESs were transparent to slightly yellow in colour, and were very viscous liquids with densities ranging between 0.92–1.08 g cm^{-2} (Table 1, Fig. S1–S3†).

Spectroscopic insight into the novel DESs' structures

It is commonly accepted that DESs are hydrogen-bonded supramolecular complexes and the presence of these bonds is responsible for the formation and stability of these systems.[39] To study the interactions between DESs' components, we used two complementary techniques, namely ^{1}H NMR and FTIR spectroscopies.

Initially, we proved by ^{1}H NMR spectroscopy (Fig. 1) that both the hydroxy- and aliphatic acids-based DESs were physical mixtures of the starting materials, and the components did not undergo any undesired side reactions during melting. The spectra of solutions of the DESs showed only the proton resonances of their constituents, shifted in some cases due to HBD–HBA intermolecular interactions.

It was reported that ^{1}H NMR can confirm the presence of hydrogen bonds in DESs, both in bulk systems as well as in mixtures with D_2O (which could disrupt the supramolecular structure).[39,40] It is well known that hydrogen bonding shifts the resonance signal of a proton to lower field (higher frequency). The ^{1}H NMR spectrum of ([EMIm]Cl) : HAs (Fig. S8†) showed that the protons in the imidazole ring experienced significant upfield shifts from 7.55 and 10.42 ppm to 7.38 and 10.12 ppm, respectively (see Fig. 1A, marked by bullet and triangular symbols). Furthermore, the labile hydroxy proton of HAs was shifted from 6.75 to 5.05 ppm. The upfield shifts in ([EMIm]Cl) : 2HAs DES (Fig. S9†) were greater than in ([EMIm]Cl) : HAs (Fig. S8†), suggesting the formation of stronger hydrogen bonds. In the spectrum of DESs prepared from aliphatic acids as a HBD, the upfield shift was visible only for signals from imidazole ring protons (see Fig. 1B, marked by bullet and triangular symbols).

The spectra of ([TBMA]Cl) : Has (Fig. S10†) and ([TBMA]Cl) : 2HAs (Fig. S11†) exhibited small shifts of the signals in comparison with the spectra of the individual DESs' com-

Table 1 Densities and viscosities measured for DESs at 60 °C

DESs	Density, ρ [g cm^{-3}]	Kinetic viscosity, η [mPa s]	Dynamic viscosity, ν [mm^2 s^{-1}]
([EMIm]Cl) : Aliph	1.0166	20.80	20.46
([EMIm]Cl) : 2Aliph	0.9728	19.84	20.39
([TBMA]Cl) : Aliph	0.9312	69.50	74.63
([TBMA]Cl) : 2Aliph	0.9230	47.78	51.77
([EMIm]Cl) : HAs	1.0784	123.26	114.30
([EMIm]Cl) : 2HAs	1.0443	51.18	49.01
([TBMA]Cl) : HAs	0.9710	103.80	105.80
([TBMA]Cl) : 2HAs	0.9815	220.18	226.80
([Ch]Cl) : 2HAs	1.0504	—	—

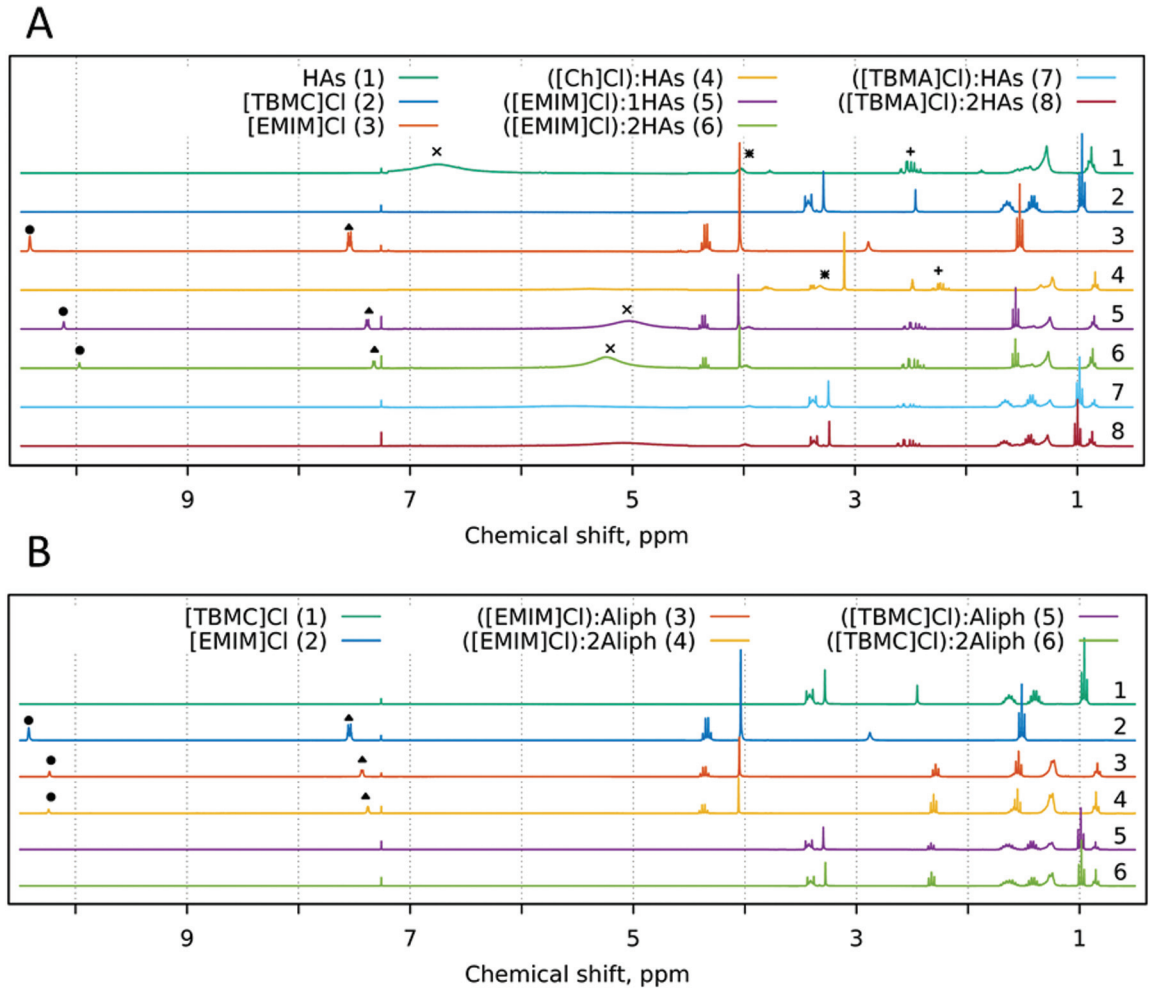

Fig. 1 ^{1}H NMR spectra of HAs-based DESs and their pure components (Panel A) and Aliph-based DESs and their pure components (Panel B). The range between 7.2 and 4.5 ppm is magnified ten times to better visualise the broad hydroxy proton resonances. For signals assignment, see the ESI.†

ponents. Thus, the ^{1}H NMR spectrum of ([TBMA]Cl) : 2HAs showed upfield shifted signals of protons attached to the carbons adjacent to the nitrogen atom $C\underline{H}_3$–N–$(C\underline{H}_2)_3$– from 3.28 and 3.42 ppm to 3.23 and 3.37 ppm, respectively. The proton on C3 in the HAs was shifted from 4.03 to 3.98 ppm. In the ([TBMA]Cl) : Has, we observed signal shifts of the same protons. Interestingly, the hydroxy proton signals were not present on both [TBMA]Cl-based DESs spectra.

Finally, the ^{1}H NMR spectrum of ([Ch]Cl) : 2HAs (Fig. S12†) showed that the protons between carboxylic and hydroxy groups as well as the proton adjacent to the hydroxy moiety were shifted from 2.51 and 4.04 to 2.23 and 3.04 ppm, respectively (see Fig. 1A, marked by cross and asterisk symbols). This might be a result of intermolecular ChCl–HAs interactions, or a solvent effect of DMSO-d6 on the chemical shifts.

The formation of H bonds between quaternary ammonium chlorides and carboxylic HBDs was also confirmed by FTIR by shape changes and shifts in the ranges characteristic for the given chemical compounds.[41] We prepared and analysed the spectra for the single components of the newly synthesised DESs, which can be found in the ESI.† Further, we used infrared spectroscopy to visualise the new hydrogen-bond formation in our new systems. First, we observed a characteristic red-shift due to a shift of CH_2–CH_2–O, from 1092 to 1082 cm^{-1} for ([Ch]Cl) : 2HAs[42] (Fig. S17†). This shift corresponded to the reduction of the intermolecular hydrogen bonds present in the choline chloride and the formation of new hydrogen bonds. Second, we observed blue-shifts in the DES spectra for the stretching vibrations of the C=O groups, *e.g.* for ([Ch]Cl) : 2HAs, from 1707 to 1716 cm^{-1} (Fig. S17†). Zhu *et al.* observed a similar blue-shift when aliphatic fatty acids were used as DES components and further postulated that carboxylic acids in the liquid phase form dimers, and as the carbon chain length of the carboxylic acid increases, the hydrogen bond of the two molecules of the acids becomes stronger.[42] The strong hydrogen bond created between the acid molecules was changed to a weak bond between the DES components. For other DESs, we also observed the blue-shifts,

which resulted from the reduction of intramolecular hydrogen bonds. For ([EMIm]Cl) : HAs, ([EMIm]Cl) : 2HAs, ([TBMA]Cl) : HAs and ([TBMA]Cl) : 2HAs, blue-shifts were observed from 1707 cm^{-1} for hydroxycarboxylic acids to 1716, 1716, 1716 and 1720 cm^{-1}, respectively (Fig. S18 and S19†). Similar results were also observed for DESs, which were composed of carboxylic acids. For ([EMIm]Cl) : Aliph, ([EMIm]Cl) : 2Aliph, ([TBMA]Cl) : Aliph and ([TBMA]Cl) : 2Aliph, blue-shifts were observed from 1713 to 1716, 1716, 1716 and 1723 cm^{-1}, respectively (Fig. S20 and S21†).

The hydrogen bonds had a significant effect on the OH stretching vibrations for (*R*)-3-hydroxycarboxylic acids. In all the prepared mixtures in which the hydrogen bond donors were HAs characteristic we noticed bigger red-shifts. This may have been due to the stronger involvement of HAs in hydrogen-bonding interactions with hydrogen-bond acceptors through the hydroxyl group located on the third position of the aliphatic chain. For ([Ch]Cl) : 2HAs, ([EMIm]Cl) : HAs, ([EMIm]Cl) : 2HAs, ([TBMA]Cl) : HAs and ([TBMA]Cl) : 2Has, red-shifts were observed from ~3392 cm^{-1} for hydroxycarboxylic acids to ~3314, ~3312, ~3326, ~3299 and ~3334 cm^{-1}, respectively (Fig. S17–S19†). The red-shifts also indicated the creation of more stable interactions between the DESs' components. The IR spectra of hydroxylated carboxylic acids underwent changes in the vibration states of molecules, similarly to other hydroxylcontaining compounds.[43]

The generation of intermolecular hydrogen bonds could also be demonstrated by shifts associated with the vibrations of CH_2 and CH_3 groups. In the case of ([EMIm]Cl) DESs, we observed changes of the peaks' shape and shifts of the imidazole rings. Moreover, in the case of ([EMIm]Cl), the interaction was preferred with the C–H groups closest to the nitrogen atom.[44] Therefore, we were interested in the shifts of the methylene bonds (CH2). Analysis revealed blue-shifts of the C4-H and C2-H. For ([EMIm]Cl) : HAs, ([EMIm]Cl) : 2HAs, ([EMIm]Cl) : Aliph and ([EMIm]Cl) : 2Aliph, the shifts were as follows: from ~3140 and ~3068 cm^{-1} for ([EMIm]Cl) to ~3145 and ~3075 cm^{-1}; ~3148 and ~3087 cm^{-1}; ~3145 and ~3074 cm^{-1}; ~3144 and ~3075 cm^{-1}, respectively (Fig. S18 and S20†). Additionally, for ([EMIm]Cl)-based DESs, we noticed characteristic shifts corresponding to N–H bonding at 1550–1570 cm^{-1}. We observed a similar phenomenon for ([TBMA]Cl)-based DESs, whereby red-shifts occurred for ([TBMA]Cl) : HAs, ([TBMA]Cl) : 2HAs, ([TBMA]Cl) : Aliph and ([TBMA]Cl) : 2Aliph from ~3438 to ~3295, ~3322, ~3409 and ~3405 cm^{-1}, respectively (Fig. S19 and S21†).

Based on the above-described results, we can conclude that the formation of intermolecular hydrogen bonds in DESs based on choline chloride was involved through the hydroxyl group derived from choline chloride and the hydroxyl and carboxyl groups of (*R*)-3-hydroxycarboxylic acids. In the case of the other DESs, to determine which compounds were characterised by a higher strength of newly formed hydrogen bonds, one can consider a postulate formed by Cao *et al.*, in which they state that the higher the red-shift observed, the stronger the hydrogen bond would be.[45] In our case, an exception to the rule was in the case of ([EMIm]Cl) : 2HAs, which was probably characterised by a higher hydrogen bond strength compared to ([EMIm]Cl) : HAs, based on the data analysed.

Polarity of the DESs

We used Nile Red (NR) dye for determination of the hydroxylated- and aliphatic acids-based DESs' polarities. It is well known that in contrast to Reichardt's dye, NR is uniquely stable in acidic media,[46] and the absorbance maximum shift is less sensitive to acidic solvents, such as acidic DESs.[37] As can be seen (Table S1†), the values of E_T(NR) for the investigated DESs were very similar to each other and were in the range of 51.2 (([Ch]Cl) : 2HAs) to 52.3 ([EMIm]Cl) : Aliph). As expected, the DESs were less polar in comparison to deep eutectic systems based on short-chain carboxylic acids or sugars (E_T(NR) = 44–49).[47] Our data indicate that the polarities of hydroxylated- and aliphatic acids-based DESs were close to typical organic solvents; for instance, acetic acid (51.3), methanol and dimethyl sulfoxide (52.0),[46] as well as close to the polarities of [Ch]Cl–glycerol 1 : 1 mol (50.9)[48] or [Ch]Cl–propanediol 1 : 2 mol (50.7)[49] DESs.

Thermal properties of the DESs

The melting temperatures and the beginning of thermal decomposition are among the most important properties that determine the use of a particular DES as an alternative to traditional solvents. These parameters determine the temperature range in which a deep eutectic solvent can maintain its liquid form and, consequently, the scope of its application.

We performed differential scanning calorimetry for the synthesised DESs and their components (see ESI, Fig. S23† for the *R*-3-hydroxyacid-based DESs and Fig. S24† for thermograms of the aliphatic-based DESs). First, we analysed the hydroxylated DESs. For HAs, there were two broad exothermic peaks and one endothermic peak observed on the solidification and melting curve, respectively. We could see that the onset temperature of melting was about 18 °C. The addition to the HAs of the alkylammonium ([TBMA]Cl), ([Ch]Cl), or imidazolium ([EMIm]Cl) salts had a great impact on the thermophysical properties of the DESs formed. The DSC scans presented almost flat lines, and in the range from −60 °C to 60 °C, no thermal events were observed. It could be speculated that at a higher scan rate and/or at lower temperature, a glass transition might have been observed.

Consecutively, we analysed the DESs based on aliphatic fatty acids. The DSC curves of the pure components, namely C7 and C9, agreed with the published data.[50] One melting and one crystallisation process were observed for C7, whereas for C9, in spite of melting and crystallisation, an additional solid–solid phase transition could be seen. The aliphatic acids C7 and C9 were miscible in a liquid state, but formed two separated crystal phases upon cooling. The binary phase diagram showed an eutectic point at 48 mol% of C7 and 2 °C.[50] Mixtures of C7, C9 and the organic salts ([TBMA]Cl) and ([EMIm]Cl) exhibited complex thermal behaviour, and it was obvious that detailed separate studies, using DSC, XRD and

hot-stage microscopy, would be needed to fully understand the behaviour. However, at this stage it could be safely assumed that the addition of the salts decreased the temperatures of the thermal events of the mixtures, and this effect was especially visible for ([TBMA]Cl) : 2Aliph and ([EMIm]Cl) : 2Aliph DESs.

Analysis of the TGA curves revealed that in the case of the DESs, with the exception of ([Ch]Cl) : 2HAs, a one-stage process of sample decomposition occurred (see ESI for the raw data, Fig. S25–S29†). Further analysis may suggest (by DTG) a more detailed degradation sequence of the components (Table 2).

By analysing the DTG curves of the DESs composed of ([EMIm]Cl), we can propose the following mechanism for the one-stage thermal degradation processes (Fig. S25 and S26†). The first step may be the evaporation of acids from the mixture. This process proceeded at the highest rate at temperature T_{DTG1}. The temperatures observed coincide with the available literature data for heptanoic (T_{boil} = 223 °C), nonanoic (T_{boil} = 255 °C) and (*R*)-3-hydroxyheptanoic acid (T_{boil} = 266 °C). The T_{boil} for (*R*)-3-hydroxynonanoic acid was not found; however, it is known that the boiling points of analogues from the same group increase with the chain length. Therefore, knowing the temperatures for hydroxylated heptanoic and dodecanoic (T_{boil} = 343 °C) acids, we could assume the hydroxylated nonanoic acid has a boiling point of 290–310 °C. In the next stage, the degradation of ([EMIm]Cl) would possibly take place, by dissociation, where the products are the corresponding $EMIm^+$ ions and methyl halide, occurring at a maximal rate at T_{DTG2}. Further, the imidazole ring was completely broken as proposed by Efimowa *et al.*,[51] with the greatest rate at T_{DTG3}.

In the case of the DESs composed of aliphatic acids and ([TBMA]Cl), we could propose a similar mechanism (Fig. S27 and S28†). First, organic acids may vaporise, with the maximum rate at T_{DTG1}, followed by the degradation of ([TBMA]Cl), similarly with the highest rate at T_{DTG2}. This is due to a β-elimination reaction leading to the breakdown of the cation to the ammonium and aliphatic hydrocarbons.[52] When it comes to the DESs constructed from ([TBMA]Cl) and (*R*)-3-hydroxyalkanoic acids, we observed an interesting dependence. In the case of these mixtures, the boiling point of the acids may be higher than the end temperature of the ([TBMA]Cl)-based DES decomposition ($T_{99\%}$). Therefore, we can assume that decomposition of these compounds occurs in the reverse order, *i.e.* initially, TBMA T_{DTG1} degradation is presumed to occur, followed by acid evaporation at T_{DTG2}. In the case of the choline-based DES degradation, a two-stage process is associated with adsorbed water. Kadhom *et al.* observed a similar relationship, whereby the rate of the onset of decomposition increased with growing water content. This was due to the priority of water evaporation before the choline-based DESs degradation[53] (Fig. S29). Therefore, it can be concluded that the decomposition of DESs based on choline chloride began at 196 °C (T_{ONSET}).

When analysing the DESs containing 1-ethyl-3-methylimidazolium chloride and choline chloride, we noticed a decrease in the onset temperature of thermal degradation (T_{onset}), when compared to the ionic liquid used. A similar relationship was observed for DESs based on choline chloride and other hydrogen carboxylic acid donors, *i.e.* levulinic acid (T_{boil} = 245 °C), phenylacetic acid (T_{boil} = 265 °C) and phenylpropionic acid (T_{boil} = 279 °C).[54] As presented in Table 2, when the content of (*R*)-3-hydroxycarboxylic acids was increased in the mixtures, the decomposition temperature (T_{ONSET}) also increased. As for the mixtures in which the acid had a lower boiling point than the temperature of the end of the DES degradation, *e.g.* ([EMIm]Cl) : HAs, we observed the opposite effect on thermal stability. The thermal stability of the DESs prepared from the (*R*)-3-hydroxycarboxylic acids was characterised by a slightly increased stability compared to their aliphatic analogues, and this enables wider possible applications. In all the analysed groups of DESs (*e.g.* ([TBMA]Cl) : HAs and ([TBMA]Cl) : 2HAs), regardless of the ratio of hydrogen donors and acceptors, we observed a similar temperature for 99% weight loss.

Wetting properties of the DESs

Measurements of liquid contact angles on solid surfaces are an important tool for characterising the degree of adhesion

Table 2 Thermogravimetric analysis of the DESs and their components

	T_{ONSET} [°C]	T_{ONSET2} [°C]	T_{DTG1} [°C]	T_{DTG2} [°C]	T_{DTG3} [°C]	Δm 99%	Weight loss up to 150 °C [%]
([EMIm]Cl)	245	—	291	311	—	328	1.0
([Ch]Cl)	97	196	282	—	—	344	2.0
([TBMA]Cl)	190	—	232	—	—	255	2.0
HAs	155	—	272	—	—	292	4.4
Aliph	177	—	246	—	—	253	1.5
([EMIm]Cl) : Aliph	192	—	251	282	302	317	1.2
([EMIm]Cl) : 2Aliph	196	—	251	277	300	310	1.2
([TBMA]Cl) : Aliph	205	—	249	—	—	271	1.2
([TBMA]Cl) : 2Aliph	206	—	252	—	—	272	0.9
([EMIm]Cl) : HAs	230	—	272	293	—	318	1.2
([EMIm]Cl) : 2HAs	206	—	267	287	311	321	3.2
([TBMA]Cl) : HAs	203	—	242	272	—	288	3.0
([TBMA]Cl) : 2HAs	213	—	264	275	—	287	2.6
([Ch]Cl) : 2HAs	97	197	269	—	—	345	2.6

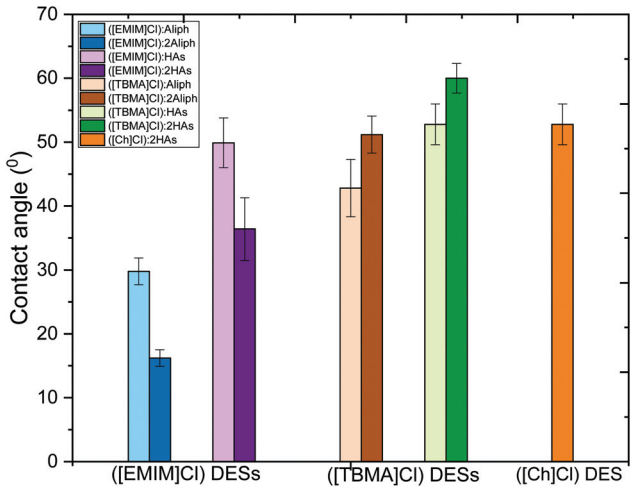

Fig. 2 Contact angles of the prepared DESs.

and the wettability of liquids on a solid surface.[55] We obtained the experimental values for the contact angles of the investigated DESs at 22 °C (Fig. 2). The wetting angles with a Teflon surface for ([EMIm]Cl)–aliphatic acids-based DESs were 29.8 ± 2.1° and 16.2 ± 1.3° for equimolar and 1 : 2 molar ratios, respectively. When (*R*)-3-hydroxycarboxylic acids were used as hydrogen donors, we observed increased contact angle values for the analogues (49.5 ± 2.6° and 36.4 ± 4.9°, respectively). In the case of ([TBMA]Cl)-based DESs an inverse relationship was observed. One can notice a general relationship that by increasing the ratio of the donor to acceptor in the case of DESs based on ([TBMA]Cl), the contact angle measurement on Teflon surfaces increased. However, ([TBMA]Cl)-based DESs showed higher values for the contact angles, revealing their more hydrophilic character. The wettability of a Teflon surface for ([TBMA]Cl)–aliphatic acids-based DESs were 42.8 ± 4.5° and 51.2 ± 2.9° for ([TBMA]Cl) : Aliph and ([TBMA]Cl) : 2Aliph, respectively. When (*R*)-3-hydroxycarboxylic acids were used as hydrogen donors, the contact angles were 52.8 ± 3.2° and 60.0 ± 2.3° for equimolar and 1 : 2 molar ratios, respectively. For choline chloride-based DESs, a contact angle of 55.9 ± 3.3° was observed. The hydrophilicity of DESs based on choline chloride and tributylmethylammonium chloride can be justified by the properties of the cation used to construct these DESs. Both cations are often used as components of surfactants.[56,57] Generally, the increase in the basicity of hydrogen bond in DESs leads to higher contact angles on a non-polar surface, such as Teflon, thus reducing the wetting ability of this surface.[58,59] In our case, the least basic alkalinity of hydrogen bond was represented in the ([EMIm]Cl)-based DESs, thus they proved to have the most hydrophobic properties.

Biodegradability and cytotoxicity of the DESs

Features such as the biodegradability and cytotoxicity of novel solvents are important parameters that influence their usability in particular applications. Here, we conducted studies in order to determine whether the newly synthesised DESs are easily decomposed in the environment and whether they bare any cytotoxicity against fibroblast cells. First, we submitted each of the synthesised DESs to biodegradation studies with activated sludge over the period of 21 days. HBDs (both aliphatic and hydroxylated fatty acids) were decomposed within 5 to 6 days in each of the tested DESs, as analysed by HPLC-MS (Fig. S30 and S31†). However, neither ([TBMA]Cl) nor ([EMIm]Cl) HBAs were degraded during the course of the experiment. Promisingly, the DES based on choline chloride and hydroxylated fatty acid was biodegraded fully already after 5 days of incubation (Fig. 3A). It is well known that choline chloride, simple organic acids and (*R*)-3-hydroxyacids are well biodegradable,[60,61] whereas ([TBMA]Cl) and ([EMIm]Cl) only reluctantly degrade in nature,[62] thus our results are in line with current state of the art.

Subsequent cytotoxicity tests revealed a moderate toxicity of the DESs based on either ([TBMA]Cl) or ([EMIm]Cl) to the fibroblast cells. The IC_{50} values for the aliphatic or hydroxylated fatty acids for (([TBMA]Cl)-based DESs) were within the

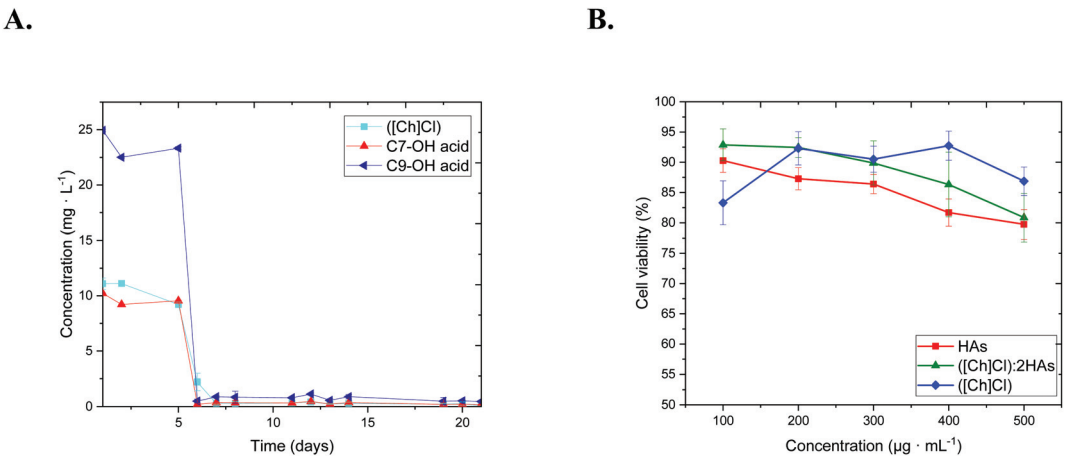

Fig. 3 A. Biodegradation of prepared choline chloride-based DES; B. Cell viability MEF 3T3 cells after 24 h of exposure to different concentrations of prepared choline chloride-based DES, (*R*)-hydroxyacids and choline chloride.

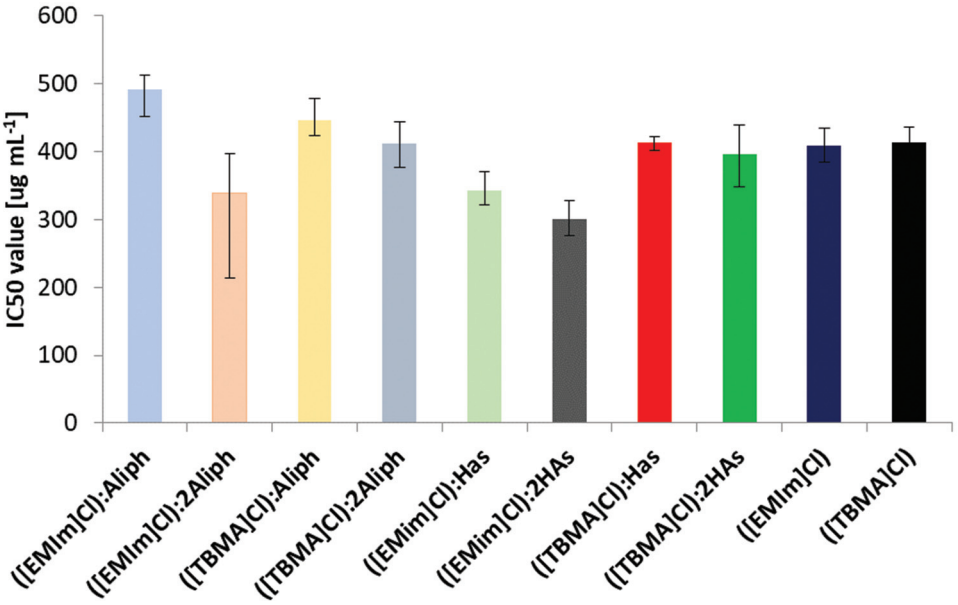

Fig. 4 Inhibitory concentration values (IC_{50}) for the prepared DESs. IC_{50} values are expressed as an average of 3 independently replicated experiments. **For aliphatic acids, (*R*)-hydroxy acids, choline chloride and the prepared DES–([Ch]Cl) : 2Has, the obtained values were $IC_{50} \gg 500$ μg ml^{-1}.**

Table 3 Solubility of lignin in the DESs at 50 °C (mg mL^{-1})

	HBA (1 mol)		
HBD	([TBMA]Cl)	([EMIm]Cl)	([Ch]Cl)
HAs (1 mol)	0.6	0.8	—
HAs (2 mol)	0.9	26.9	25.6
Aliph (1 mol)	7.2	29.8	—
Aliph (2 mol)	15.6	30.7	—

Lignin solubility was also tested in DES building fatty acids and other typical solvents; the values in parentheses are in mg mL^{-1} – aliph (0.2), HAs (0.3), water (>100.0), DMSO (20.0) and methanol (7.0).

standard deviation of the hydrogen-bond acceptor used (Fig. 4 and Fig. S32†). Aliphatic ([EMIm]Cl)-based DESs in 2 : 1 mol : mol HBD to HBA ratios revealed similar IC_{50} values to this obtained for hydroxylated DESs (281 μg ml^{-1} *vs.* 272 μg ml^{-1}); however, when the molar ratio was decreased to 1 : 1 (HBA to HBD), the IC_{50} value was higher by 1.5-fold for the hydroxylated ([EMIm]Cl) DES (Fig. 4 and Fig. S32†). In general, for these two HBAs, namely ([TBMA]Cl) and ([EMIm]Cl), aliphatic DESs were characterised with higher IC_{50} values. When DESs were constructed with choline chloride, they did not reveal any cytotoxicity in the tested range ($IC_{50} \gg 500$ μg ml^{-1}, Fig. 3B), which in turn confirms their environmental friendliness.

Application example: lignin solubilisation

Lignocellulosic biomass is the world's most abundant renewable resource. It consists primarily of cellulose, hemicellulose and lignin.[63] These compounds, through bioprocessing in biorefineries, can be converted into many valuable products, ranging from simple fermentation feedstocks to advanced biomaterials.[64] However, there is still scope for providing bioindustries with environmental friendly, efficient and selective solvents for the extraction of a given lignocellulosic fraction. We tested our constructed DESs for this purpose on model substances. The prepared solvents were not able to solubilise cellulose; however, they proved to be good solubilising agents for lignin. The best performing solvents were those based on ([EMIm]Cl) cation and aliphatic fatty acids (60.8% and 80.4% of lignin solubilisation, Table 3). When ([EMIm]Cl) and ([TBMA]Cl) were supplemented with HAs, only ([EMIm]Cl) : 2HAs enabled 49.5% solubilisation of lignin. However, from a green perspective, the most promising result was obtained for the DES based on choline chloride and hydroxyacids; here a 43.6% solubilisation of lignin was demonstrated. As stated above, this particular DES was shown to be readily biodegradable and demonstrated no cytotoxicity against mammalian cells. Therefore, the application of DESs based on ([Ch]Cl) and (*R*)-3-hydroxyacids for lignin extraction from biomass seems a green alternative to the currently used solvents for these purposes. Moreover, there are more than 150 different (*R*)-3-hydroxyacids synthesised by bacteria into polyhydroxyalkanoate polymers;[65] therefore, the possibilities of constructing appropriate DESs for a particular purpose have a high probability.

Conclusions

Bacteria are able to synthesise PHA polymers from numerous carbon sources of different origins, *i.e.* biomass derived (*i.e.* fatty acids, glycerol, sugars, phenols), waste derived (*i.e.* chemically altered synthetic polymers, municipal solid wastes, wastewaters, pollutants, such as methanol) and even gaseous sub-

strates (carbon monoxide, carbon dioxide). PHA-synthesising microorganisms convert these substances *via* complex biochemical processes to enantiopure (*R*)-3-hydroxylated fatty acids that further are polymerised into PHA molecules, which enable bacteria to survive hard environmental conditions. Years of PHA research have brought numerous applications for PHA polymers and their monomers – HAs. However, to the best our knowledge, this is a first proof-of-concept report that employs HAs in the construction of deep eutectic solvents. In parallel to ([EMIm]Cl)- and [TBMA]Cl-based DESs, we demonstrated that a given mixture of HAs derived from polyhydroxynonanoate enables the synthesis of natural DESs with choline chloride as a hydrogen-bond acceptor. An in-depth characterisation of each synthesised DES was performed that allowed us to describe the intramolecular interactions alongside several physical parameters of these new solvents. Further, we showed that DESs based on choline chloride and bacterially derived monomers of PHA are fully biodegradable and are not cytotoxic. Moreover, we also demonstrated the usability of HAs-based DESs as potential alternatives for lignin solubilisation. We believe that in the near future new members belonging to this new family of natural DESs will be constructed based on HAs derived from so far underutilised biomass resources (*i.e.* waste glycerol from biodiesel production, post frying waste fatty acids). This plausible path could lead to the generation of a series of solvents that are environmentally friendly and that enable the upcycling of bioresources.

Conflicts of interest

There are no conflicts to declare.

Acknowledgements

This research was funded by the statutory research fund of ICSC PAS. Katarzyna Haraźna and Wojciech Snoch acknowledge the support of InterDokMed project no. POWR.03.02.00-00-I013/16. The authors are grateful to Joanna Ortyl and Paweł Fiedor for the help with DSC measurements, Joanna Kryściak-Czerwenka for IR measurements, Daria Solarz and Olga Adamczyk for performing part of the cytotoxicity studies, and Anna Miłaczewska for creation of graphical abstract. We greatly acknowledge the joint consortium "Interdisciplinary Centre of Physical, Chemical and Biological Sciences" of ICSC PAS and INP PAS for providing the access to Agilent 1290 Infinity System with automatic autosampler and MS Agilent 6460 Triple Quad Detector.

References

1 P. Pollet, E. A. Davey, E. E. Ureña-Benavides, C. A. Eckert and C. L. Liotta, *Green Chem.*, 2014, **16**, 1034–1055.
2 L. Moity, M. Durand, A. Benazzouz, C. Pierlot, V. Molinier and J.-M. Aubry, *Green Chem.*, 2012, **14**, 1132.
3 E. L. Smith, A. P. Abbott and K. S. Ryder, *Chem. Rev.*, 2014, **114**, 11060–11082.
4 A. Paiva, R. Craveiro, I. Aroso, M. Martins, R. L. Reis and A. R. C. Duarte, *ACS Sustainable Chem. Eng.*, 2014, **2**, 1063–1071.
5 Y. Liu, J. B. Friesen, J. B. McAlpine, D. C. Lankin, S.-N. Chen and G. F. Pauli, *J. Nat. Prod.*, 2018, **81**, 679–690.
6 C. Florindo, L. C. Branco and I. M. Marrucho, *ChemSusChem*, 2019, **12**(8), 1549–1559.
7 Y. H. Choi, J. van Spronsen, Y. Dai, M. Verberne, F. Hollmann, I. W. C. E. Arends, G.-J. Witkamp and R. Verpoorte, *Plant Physiol.*, 2011, **156**, 1701–1705.
8 Y. Dai, J. van Spronsen, G.-J. J. Witkamp, R. Verpoorte and Y. H. Choi, *Anal. Chim. Acta*, 2013, **766**, 61–68.
9 D. J. G. P. van Osch, L. F. Zubeir, A. van den Bruinhorst, M. A. A. Rocha and M. C. Kroon, *Green Chem.*, 2015, **17**, 4518–4521.
10 B. D. Ribeiro, C. Florindo, L. C. Iff, M. A. Z. Coelho and I. M. Marrucho, *ACS Sustainable Chem. Eng.*, 2015, **3**, 2469–2477.
11 J. D. Mota-Morales, R. J. Sánchez-Leija, A. Carranza, J. A. Pojman, F. del Monte and G. Luna-Bárcenas, *Prog. Polym. Sci.*, 2018, **78**, 139–153.
12 F. Del Monte, D. Carriazo, M. C. Serrano, M. C. Gutiérrez and M. L. Ferrer, *ChemSusChem*, 2014, **7**, 999–1009.
13 E. Durand, J. Lecomte and P. Villeneuve, *Eur. J. Lipid Sci. Technol.*, 2013, **115**, 379–385.
14 H. Zhao, C. Zhang and T. D. Crittle, *J. Mol. Catal. B: Enzym.*, 2013, **85–86**, 243–247.
15 G. Young, F. Nippgen, S. Titterbrandt and M. J. Cooney, *Sep. Purif. Technol.*, 2010, **72**, 118–121.
16 J. Cao, L. Chen, M. Li, F. Cao, L. Zhao and E. Su, *Green Chem.*, 2018, **20**, 1879–1886.
17 M. Yang, J. Cao, F. Cao, C. Lu and E. Su, *Chem. Biochem. Eng. Q.*, 2018, **32**, 315–324.
18 M. W. Nam, J. Zhao, M. S. Lee, J. H. Jeong and J. Lee, *Green Chem.*, 2015, **17**, 1718–1727.
19 R. Davis, R. Kataria, F. Cerrone, T. Woods, S. Kenny, A. O'Donovan, M. Guzik, H. Shaikh, G. Duane, V. K. Gupta, M. G. Tuohy, R. B. Padamatti, E. Casey and K. E. O'Connor, *Bioresour. Technol.*, 2013, **150**, 202–209.
20 F. Cerrone, S. K. Choudhari, R. Davis, D. Cysneiros, V. O'Flaherty, G. Duane, E. Casey, M. W. Guzik, S. T. Kenny, R. P. Babu and K. O'Connor, *Appl. Microbiol. Biotechnol.*, 2014, **98**, 611–620.
21 J. Nikodinovic-Runic, M. Guzik, S. T. Kenny, R. Babu, A. Werker and K. E. O. Connor, in *Advances in Applied Microbiology*, 2013, vol. 84, pp. 139–200.
22 M. W. Guzik, S. T. Kenny, G. F. Duane, E. Casey, T. Woods, R. P. Babu, J. Nikodinovic-Runic, M. Murray and K. E. O'Connor, *Appl. Microbiol. Biotechnol.*, 2014, **98**, 4223–4232.
23 T. Witko, M. Guzik, K. Sofińska, K. Stepien and K. Podobinska, *Biophys. J.*, 2018, **114**, 363a.
24 R. P. Babu, K. O. Connor and R. Seeram, *Prog. Biomater.*, 2013, **2**, 8.

25 J. Staroń, J. M. Dąbrowski, E. Cichoń and M. Guzik, *Crit. Rev. Biotechnol.*, 2017, 1–14.
26 E. Liwarska-Bizukojc, C. Maton and C. V. Stevens, *Biodegradation*, 2015, **26**, 453–463.
27 S. Zhu, J. Zhou, H. Jia and H. Zhang, *Food Chem.*, 2018, **243**, 351–356.
28 J. Cao, M. Yang, F. Cao, J. Wang and E. Su, *ACS Sustainable Chem. Eng.*, 2017, **5**, 3270–3278.
29 J. Cao, M. Yang, F. Cao, J. Wang and E. Su, *J. Cleaner Prod.*, 2017, **152**, 399–405.
30 W. Tang, Y. Dai and K. H. Row, *Anal. Bioanal. Chem.*, 2018, **410**, 7325–7336.
31 X.-D. Hou, Q.-P. Liu, T. J. Smith, N. Li and M.-H. Zong, *PLoS One*, 2013, **8**, e59145.
32 S. Dubey, P. Bharmoria, P. S. Gehlot, V. Agrawal, A. Kumar and S. Mishra, *ACS Sustainable Chem. Eng.*, 2018, **6**, 766–773.
33 Y. H. Kim, Y. K. Choi, J. Park, S. Lee, Y. H. Yang, H. J. Kim, T. J. Park, Y. Hwan Kim and S. H. Lee, *Bioresour. Technol.*, 2012, **109**, 312–315.
34 K. M. Docherty, M. V. Joyce, K. J. Kulacki and C. F. Kulpa, *Green Chem.*, 2010, **12**, 701–712.
35 K. Sofińska, J. Barbasz, T. Witko, J. Dryzek, K. Haraźna, M. Witko, J. Kryściak-Czerwenka and M. Guzik, *J. Appl. Polym. Sci.*, 2019, **136**, 47192.
36 J. Radivojevic, S. Skaro, L. Senerovic, B. Vasiljevic, M. Guzik, S. T. Kenny, V. Maslak, J. Nikodinovic-Runic and K. O'Connor, *Appl. Microbiol. Biotechnol.*, 2015, **100**, 161–172.
37 G. Imperato, S. Höger, D. Lenoir and B. König, *Green Chem.*, 2006, **8**, 1051–1055.
38 C. Tamm, S. P. Galitó and C. Annerén, *PLoS One*, 2013, **8**, 1–10.
39 C. R. Ashworth, R. P. Matthews, T. Welton and P. A. Hunt, *Phys. Chem. Chem. Phys.*, 2016, **18**, 18145–18160.
40 M. C. Gutiérrez, M. L. Ferrer, C. R. Mateo and F. Del Monte, *Langmuir*, 2009, **25**, 5509–5515.
41 N. Asprion, H. Hasse and G. Maurer, *Fluid Phase Equilib.*, 2001, **186**, 1–25.
42 W. Zhu, C. Wang, H. Li, P. Wu, S. Xun, W. Jiang, Z. Chen, Z. Zhao and H. Li, *Green Chem.*, 2015, **17**, 2464–2472.
43 W. Guo, Y. Hou, W. Wu, S. Ren, S. Tian and K. N. Marsh, *Green Chem.*, 2013, **15**, 226–229.
44 P. A. Hunt, C. R. Ashworth and R. P. Matthews, *Chem. Soc. Rev.*, 2015, **44**, 1257–1288.
45 L. Cao, J. Huang, X. Zhang, S. Zhang, J. Gao and S. Zeng, *Phys. Chem. Chem. Phys.*, 2015, **17**, 27306–27316.
46 J. F. Deye, T. A. Berger and A. G. Anderson, *Anal. Chem.*, 1990, **62**, 615–622.
47 K. O. Wikene, H. V. Rukke, E. Bruzell and H. H. Tønnesen, *Eur. J. Pharm. Biopharm.*, 2016, **105**, 75–84.
48 Y. Huang, F. Feng, J. Jiang, Y. Qiao, T. Wu, J. Voglmeir and Z. G. Chen, *Food Chem.*, 2017, **221**, 1400–1405.
49 K. Mulia, S. Putri, E. Krisanti and Nasruddin, *AIP Conference Proceedings*, 2017, vol. 1823, p. 020022.
50 Z. Wang, G. Ma, S. Liu, Y. Jing, J. Sun and Y. Jia, *Energy Build.*, 2017, **145**, 259–266.
51 A. Efimova, L. Pfützner and P. Schmidt, *Thermochim. Acta*, 2015, **604**, 129–136.
52 E. Bourgeat-Lami, F. Di Renzo, F. Fajula, P. H. Mutin and T. Des Courieres, *J. Phys. Chem.*, 1992, **96**, 3807–3811.
53 M. A. Kadhom, G. H. Abdullah and N. Al-Bayati, *Arabian J. Sci. Eng.*, 2017, **42**, 1579–1589.
54 N. Delgado-Mellado, M. Larriba, P. Navarro, V. Rigual, M. Ayuso, J. García and F. Rodríguez, *J. Mol. Liq.*, 2018, **260**, 37–43.
55 K. N. Marsh, *J. Chem. Eng. Data*, 2006, **51**, 1480–1480.
56 R. Zana, J. Schmidt and Y. Talmon, *Langmuir*, 2005, **21**, 11628–11636.
57 R. Klein, M. Kellermeier, D. Touraud, E. Müller and W. Kunz, *J. Colloid Interface Sci.*, 2013, **392**, 274–280.
58 M. M. Pereira, K. A. Kurnia, F. L. Sousa, N. J. O. Silva, J. A. Lopes-Da-Silva, J. A. P. Coutinho and M. G. Freire, *Phys. Chem. Chem. Phys.*, 2015, **17**, 31653–31661.
59 G. V. S. M. Carrera, C. A. M. Afonso and L. C. Branco, *J. Chem. Eng. Data*, 2010, **55**, 609–615.
60 K. Radošević, M. Cvjetko Bubalo, V. Gaurina Srček, D. Grgas, T. Landeka Dragičević and R. I. Redovniković, *Ecotoxicol. Environ. Saf.*, 2015, **112**, 46–53.
61 T. Narancic, S. Verstichel, S. Reddy Chaganti, L. Morales-Gamez, S. T. Kenny, B. De Wilde, R. Babu Padamati and K. E. O'Connor, *Environ. Sci. Technol.*, 2018, **52**, 10441–10452.
62 A. Jordan and N. Gathergood, *Chem. Soc. Rev.*, 2015, **44**, 8200–8237.
63 D. Watkins, M. Nuruddin, M. Hosur, A. Tcherbi-Narteh and S. Jeelani, *J. Mater. Res. Technol.*, 2015, **4**, 26–32.
64 A. Elmekawy, L. Diels, H. De Wever and D. Pant, *Environ. Sci. Technol.*, 2013, **47**, 9014–9027.
65 A. Steinbüchel and H. E. Valentin, *FEMS Microbiol. Lett.*, 1995, **128**, 219–228.